Eurasian Journal of Soil Science 2024, 13(1), 26 - 34

Eurasian Journal of Soil Science

Journal homepage : http://ejss.fesss.org

Optimal timing of satellite data acquisition for estimating and modeling soil salinity in cotton fields of the Mingbulak District, Uzbekistan

Shovkat Kholdorov [a,b,*], Zafarjon Jabbarov [b], Tomoaki Yamaguchi [a], Megumi Yamashita [a], Tulkin Shamsiddinov [c], Keisuke Katsura [a]

[a] Graduate School of Agriculture, Tokyo University of Agriculture and Technology, Tokyo, Japan
[b] Department of Soil Science, National University of Uzbekistan named after Mirzo Ulugbek, Tashkent, Uzbekistan
[c] Tashkent State Agrarian University, Tashkent, Uzbekistan

Article Info
Received : 18.05.2023
Accepted : 09.10.2023
Available online : 24.10.2023

Author(s)
S.Kholdorov
Z.Jabbarov
T.Yamaguchi
M.Yamashita
T.Shamsiddinov
K.Katsura *

* Corresponding author

Abstract

Agriculture is frequently hampered by soil salinity, which has a negative impact on crop growth and yield. This study aims to identify the optimal timing of satellite data acquisition to predict soil salinity levels indirectly using satellite images in cotton growth fields as a basis. Data was collected in the Mingbulak district of Uzbekistan, where soil electrical conductivity (EC) was measured in a laboratory using soil samples collected from various fields with similar management practices. In this research, we present a linear regression model that uses satellite data and the Normalized Difference Salinity Index (NDSI) to forecast soil salinity levels indirectly. The results of the linear regression analysis showed a positive correlation between the soil electrical conductivity values and the NDSI values for each month, with August having the highest correlation (R^2 = 0.70). The study found that the cotton growth stages and the process of soil salinity formation in the study area were the main factors affecting the correlation between electrical conductivity and NDSI. The model developed in this study has R^2 value of 0.70. This suggests a moderate to strong relationship between the two variables, which is promising for the indirect assessment of soil salinity using the NDSI index. The study discovered a positive relationship between soil electrical conductivity and NDSI values, which were highest in pre-flowering and flowering stages of cotton. Our findings show that satellite-based estimation and modeling with NDSI can be used to indirectly assess cotton field soil salinity, especially during the pre-flowering and flowering stages. This study contributes to the development of optimal satellite data acquisition timing, which can improve soil salinity predictions and agricultural productivity.

Keywords: Cotton, index, soil, salinity, satellite image.

Introduction

Salinity is a pervasive issue in many arid and semi-arid regions worldwide, including Uzbekistan, where it significantly impacts crop productivity and agricultural yields (Hamad, 2016; Asfaw et al., 2018; Zörb et al., 2019). In Uzbekistan alone, saline soils affect half of the 4.2 million-hectare irrigated agricultural area (Kholdorov et al., 2022). Several factors contribute to soil salinization, such as mineralization, groundwater depth, and the imbalance between precipitation and evaporation (Stavi et al., 2021; Zhang et al., 2022). It is crucial to map and monitor soil salinity for national food security purposes. While conventional techniques for mapping and monitoring geographical and temporal changes in soil salinity exist, they may prove to be slower, more costly, and more intensive than remote sensing technologies (Tan et al., 2023). Given the substantial variability in soil salinity across large regions and timeframes, the effective mapping and monitoring of soil salinity in irrigated lands is crucial (Kholdorov et al., 2023a).

doi : https://doi.org/10.18393/ejss.1380500
: http://ejss.fesss.org/10.18393/ejss.1380500
Publisher : Federation of Eurasian Soil Science Societies
e-ISSN : 2147-4249

Remote sensing has recently become an effective approach for soil salinization mapping because of its rapid updates, large coverage, and significant spectrum information. Nevertheless, remote sensing applications are severely constrained when the soil surface is partially vegetated, since vegetation may affect the overall spectral features of saline soil, resulting in poor forecast accuracy (Liu et al., 2019). However, plant cover may be utilized as the primary indication of agricultural land salinity. Vegetation indices were utilized as indirect indicators in various investigations to demonstrate a relationship between remote sensing spectral reflectance and soil salinity (Khajehzadeh et al., 2022; Li et al., 2022). Some research has utilized salinity indices, which are strongly connected to vegetative cover, to assess cropland salinity (Aslanov et al., 2021; Kholdorov et al., 2023b). The degree of soil salinisation is intimately connected to vegetation characteristics. For example, plants may generate less chlorophyll when stressed by high soil salt levels, resulting in alterations in the reflectance spectra of leaves (Zhu et al., 2021). As plants are subjected to biotic and abiotic stress (such as salt), their photosynthetic activity diminishes, resulting in increased visible reflectance and decreased near-infrared reflectance (NIR) from the vegetation (Scudiero et al., 2015). Soil salinity has been determined in areas with different types of vegetation, including cotton vegetation (Pankova and Mazikov, 1985; Zhang et al., 2021). Cotton is considered an ideal indicator for assessing soil salinity in irrigated drylands because of its strong correlation with electrical conductivity (Metternicht and Zinck, 2003). Aerial imaging techniques are effectively employed to map and quantify soil salinity levels in cotton fields by integrating image analysis, spectral observations, and ground-truth data (Wiegand et al., 1994). Accurate estimation of salinity from satellite imagery is contingent on the temporal dimension of image data acquisition. Pankova and Mazikov (1976) established the most favorable timing for detecting salinization in cotton fields using aerial photographs as their principal data source. In Turkey, the evaluation of soil salinity relies on hyperspectral remote sensing and the spectral characteristics of crops, such as cotton and wheat, confirming their suitability for detecting soil salinity (Allbed and Kumar, 2013). Ivushkin et al. (2017) conducted a study in Uzbekistan's salt-affected semi-arid Syrdarya Province, utilizing MODIS satellite data to monitor canopy temperature. Their research revealed significant correlations between soil salinity and canopy temperature, with the most pronounced associations observed in cotton fields, particularly in September. Advancements in remote sensing technology have resulted in improved accuracy and precision for measuring soil salinity. Advanced satellite sensors can provide a precise assessment of salinity levels in cotton fields, thereby enabling efficient crop management and yield optimization. The indirect estimation of soil salinity using satellite image is relatively straightforward when studies are conducted on a variety of plant species. This is because the large variation in soil salinity that results from the diversity of the environment makes the estimation of soil salinity relatively straightforward. However, when only cotton fields are considered, the variation in soil salinity may be quite minimal. The existence of salt-tolerant weeds in cultivated fields has the potential to decrease the accuracy of indirect salinity determination as these plants are able to flourish in saline environments. Nevertheless, in the cotton fields of the study region, salt-tolerant weeds are rarely observed due to the implementation of regular weed control measures. Additionally, the study was conducted in these cotton fields because they represent over half of the agricultural land in Mingbulak district. This makes it possible to produce a district-level salinity map utilizing the developed model. Because of this, the applicability of existing methods for estimating soil salinity from remote sensing data is called into question. It is necessary to conduct additional research in order to determine whether or not such methods can be applied successfully in this context. Furthermore, the time of year when the image data used for this purpose is captured is also considered to be important in accurately estimating salinity from satellites. However, to the best of our knowledge, there are no studies that have investigated the optimal timing in Mingbulak disrtrict of Uzbekistan.

We used satellite-based estimation and modelling to fill the knowledge gap in indirect soil salinity analysis in cotton fields in Mingbulak, Uzbekistan. Our novel method uses satellite images to determine the best time to estimate soil salinity levels, improving our understanding of indirect soil salinity and plant growth. We used five months of Landsat 8 Operational Land Imager images and linear regression analysis of NDSI values from the satellite images because of based on our previous study where we compared 17 indices obtained from Landsat 8 and Sentinel-2A satellite data and found that Landsat 8 NDSI index provided highly accurate estimates of soil salinity (Kholdorov et al., 2023b). In total, we used five months of satellite imagery and collected soil samples from 40 points in the study field to verify EC values. Research questions: How well do satellite-based estimation and modeling indirectly assess soil salinity in cotton fields in Mingbulak district? When should satellite images be used to estimate indirect soil salinity in study cotton fields? We aimed to create a high-resolution remote sensing and statistical model for indirectly analyzing soil salinity. Our results will help policymakers and farmers manage indirect soil salinity in Mingbulak. This study will bridge satellite-based estimation and soil salinity analysis, improving our understanding of cotton field soil salinity dynamics.

Material and Methods

Study area

The research was carried out in Uzbekistan's Mingbulak district. The Mingbulak district is critical to the agricultural local economy (Figure 1). Irrigated cropland accounted for 37779 hectares of the total land area of 52580 ha. The majority of irrigated soil groups are represented by Gleysols or Solanchaks. The Mingbulak district is critical to the agricultural local economy. Irrigated cropland accounted for 37779 hectares of the total land area of 52580 ha. Cotton is the most important industrial crop farmed in the region.

Two soil types that are frequently found in the Minbulak district of Namangan, Uzbekistan, are gleysols and solonchaks. Poor drainage and the presence of gley and rust stains in the deeper soil layers are two characteristics of gleysols. In contrast, solonchaks are saline soils that have a high concentration of soluble salts and are typically found in arid and semiarid areas with shallow groundwater. Due to their physical and chemical characteristics, both soil groups have a restricted potential for agriculture. In the Minbulak district, where they make up the majority of irrigated soil groups, Gleysols and Solonchaks are still frequently used for irrigation. In the Minbulak district, the predominant soil types for Gleysols and Solonchaks are sandy loam, sandy clay loam, and sandy clay, with a homogeneous structure made up of layers with a light mechanical composition.

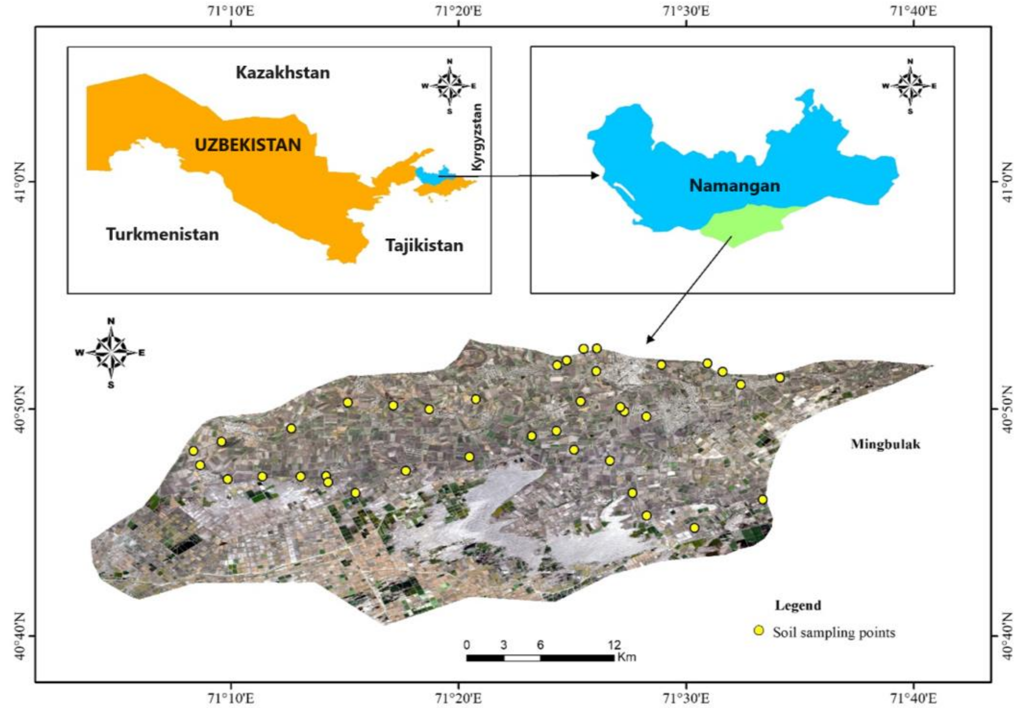

Figure 1. Study location and soil sampling points

Soil sample collection and laboratory analysis

Soil samples were collected at a depth of 0-20 cm from 40 randomly selected points in various fields with similar management practices to cotton planting in the study area from September 18 to September 25, 2022 (Figure 1). The exact coordinates of each sampling point were determined using a global positioning system (GPS).

Soil samples' EC values were determined using a soil-and-water suspension with a concentration of one-fifth (1:5). Twenty grams of air-dried soil was placed in a 250 ml polyethylene Erlenmeyer flask, 100 ml of distilled water was added (1:5, weight/volume), the flask was sealed with glass caps, and it was inverted and shaken in a horizontal position using a piston shaker. Shaken for 60 minutes at 180 osc min^{-1}. After 30 minutes of shaking, the mixture was taken out of the shaker and left to rest. The EC value (in dS m^{-1}) was determined to be optimal at a temperature of 25 degrees Celsius (FAO, 2021). The electrical conductivity values of the 1:5 soil extracts obtained in the laboratory were converted to ECe using a conversion factor specific to the soil texture of the study area to ensure consistency with the USDA classification (Richards, 1954). The conversion was carried out using the following formula, which takes into account the soil texture-specific conversion factor CF (CF = 10)

$$ECe = EC_{1:5} \times CF$$

Satellite data

As a satellite image, Landsat 8-9 Operational Land Imager (OLI) Thermal Infrared Sensor (TIRS) Collection 2 Level 2 images were used to develop a model for estimating soil salinity. The Landsat-8 image was obtained from the website (www. earth explorer.gov) of the United States Geological Survey (USGS). The Landsat 8-9 Operational Land Imager (OLI) Thermal Infrared Sensor (TIRS) Collection 2 Level images have a spatial resolution of 30 m for most bands, with a higher resolution available in the panchromatic band (15 m) and a lower resolution for thermal bands (100 m). Landsat 8-9 OLI/TRIS 2 Level data encompass visible, near-infrared, shortwave infrared, cirrus, and thermal infrared bands. They are characterized by a repeat cycle of approximately 16 days and a radiometric resolution of 12 bits per pixel. These images were preprocessed, including atmospheric correction and geometric rectification, making them ready for analysis. Landsat 8-9 OLI/TRIS 2 Level data are freely accessible and widely used for diverse applications in environmental monitoring, land cover classification, and more (Vaughn, 2019). Between May and September 2022, satellite images were obtained on five occasions at various times. On the following dates, the data was downloaded: May 24, 2022, June 25, 2022, July 27, 2022, August 20, 2022, and September 21, 2022. Band 4 (red) and band 5 (near-infrared) of Landsat 8-9 OLI/TRIS were used indirect estimating soil salinity as Normalized Difference Salinity Index (NDSI) with following equation (Khan et al., 2001).

$$\mathrm{NDSI} = (\mathrm{Red} - \mathrm{NIR})/(\mathrm{Red} + \mathrm{NIR})$$

For all five downloads, the NDSI index was calculated using the same equation and index source, with no variations or modifications. The primary reason for using the Normalized Difference Salinity Index (NDSI) as mentioned above, index determination of soil salinity in the study area is that in previous studies, the NDSI index demonstrated the highest accuracy among salinity indices (Aslanov et al., 2021; Kholdorov et al., 2023b). Using satellite images of the study area, NDSI index values were calculated using ArcGIS 10.8 software. Each soil sampling point's NDSI values were obtained separately from 5 months of satellite images.

Statistical analysis and model development

Regression analysis was carried out utilizing EC laboratory data which soil samples were taken from depths of 0-20cm. Models explaining soil EC from the NDSI salinity index obtained from the satellite were developed by a single regression analysis using the least squares method with modelling datasets. The model with the best fit was adopted by linear regression. Microsoft Excel was used for tabulation and statistical analyses. Regression analysis was performed on a cross-section of all downloaded satellite images corresponding to the cotton growing season.

Results and Discussion

Laboratory and image analysis results

Laboratory analysis and ArcGIS software were used to collect data for the study. Table 1 presents the EC values obtained by laboratory analysis of soil samples from the study area and the results obtained by processing satellite images. The soils of the study area are nonsaline (0-2 dS m^{-1}), slightly saline (2-4 dS m^{-1}), and moderately saline (4-8 dS m^{-1}) based on EC values

obtained in the laboratory and calcification suggested by USDA (Richards, 1954). The main reason for the absence of highly saline and very highly saline levels in the study area is that salt leaching measures are done every year before cotton planting. Furthermore, cotton cultivation takes place primarily in non-saline areas. Despite the fact that cotton is a relatively salt-tolerant crop, increased soil salinization would compromise its ability to cope with salt stress (Zafar et al., 2022). Cotton grown on non-saline soil has significantly higher productivity and vegetative development than cotton grown under the influence of salinization (Guo et al., 2012).

The NDSI values obtained from analyzing satellite images downloaded at five different times for the study vary considerably. NDSI values changed significantly according to the cotton growing season (Figure 2). The NDSI value was high in the first month of cotton development (May), but it dropped dramatically when cotton reached its peak of development (August). The main trend line in Figure 2 is the 36 ID soil sampled field, where the NDSI value did not change consistently due to the abundance of salt-tolerant weeds. The reasons for the change in NDSI values are discussed in detail in the statistical analysis and modeling results section.

Table 1. EC values and monthly NDSI values for each soil sampling point

ID	EC, dSm^{-1}	NDSI values					
		May	June	July	August	September	Average
1	3.25	-0.143	-0.317	-0.312	-0.303	-0.200	-0.255
2	1.22	-0.124	-0.297	-0.334	-0.387	-0.179	-0.264
3	2.23	-0.112	-0.314	-0.344	-0.337	-0.279	-0.277
4	1.2	-0.147	-0.308	-0.410	-0.419	-0.201	-0.297
5	1.82	-0.057	-0.190	-0.352	-0.328	-0.146	-0.215
6	1.38	-0.088	-0.297	-0.407	-0.408	-0.229	-0.286
7	2.3	-0.069	-0.212	-0.346	-0.360	-0.169	-0.231
8	1.27	-0.124	-0.380	-0.386	-0.394	-0.204	-0.297
9	0.86	-0.074	-0.284	-0.331	-0.372	-0.198	-0.252
10	2.29	-0.143	-0.239	-0.313	-0.335	-0.186	-0.243
11	1.75	-0.092	-0.291	-0.381	-0.400	-0.192	-0.271
12	2.07	-0.118	-0.343	-0.398	-0.425	-0.204	-0.298
13	1.6	-0.149	-0.281	-0.337	-0.356	-0.216	-0.268
14	3.05	-0.096	-0.204	-0.291	-0.340	-0.183	-0.223
15	1.64	-0.093	-0.317	-0.364	-0.368	-0.224	-0.273
16	2.18	-0.080	-0.197	-0.334	-0.310	-0.175	-0.219
17	2.38	-0.116	-0.249	-0.331	-0.360	-0.159	-0.243
18	1.58	-0.116	-0.249	-0.331	-0.360	-0.159	-0.243
19	0.42	-0.120	-0.363	-0.406	-0.429	-0.226	-0.309
20	1.29	-0.126	-0.351	-0.375	-0.390	-0.208	-0.290
21	0.49	-0.119	-0.364	-0.462	-0.460	-0.234	-0.328
22	3.3	-0.123	-0.185	-0.326	-0.311	-0.217	-0.232
23	2.01	-0.101	-0.337	-0.409	-0.420	-0.275	-0.308
24	2.36	-0.101	-0.215	-0.342	-0.343	-0.220	-0.244
25	2.25	-0.163	-0.276	-0.314	-0.338	-0.224	-0.263
26	2.04	-0.161	-0.363	-0.403	-0.414	-0.221	-0.312
27	0.75	-0.072	-0.226	-0.361	-0.392	-0.178	-0.246
28	1.16	-0.124	-0.317	-0.391	-0.410	-0.244	-0.297
29	2.36	-0.113	-0.280	-0.334	-0.346	-0.179	-0.250
30	2.24	-0.079	-0.272	-0.335	-0.348	-0.179	-0.242
31	1.9	-0.066	-0.150	-0.344	-0.332	-0.153	-0.209
32	1.43	-0.092	-0.261	-0.365	-0.384	-0.163	-0.253
33	2.21	-0.080	-0.296	-0.350	-0.384	-0.211	-0.264
34	0.5	-0.083	-0.306	-0.418	-0.433	-0.242	-0.297
35	3.26	-0.156	-0.180	-0.263	-0.296	-0.198	-0.219
36	4.5	-0.161	-0.170	-0.150	-0.160	-0.160	-0.160
37	0.42	-0.139	-0.289	-0.417	-0.422	-0.247	-0.303
38	0.46	-0.083	-0.251	-0.400	-0.425	-0.224	-0.277
39	3.18	-0.106	-0.229	-0.296	-0.332	-0.234	-0.240
40	2.19	-0.109	-0.292	-0.308	-0.358	-0.231	-0.260

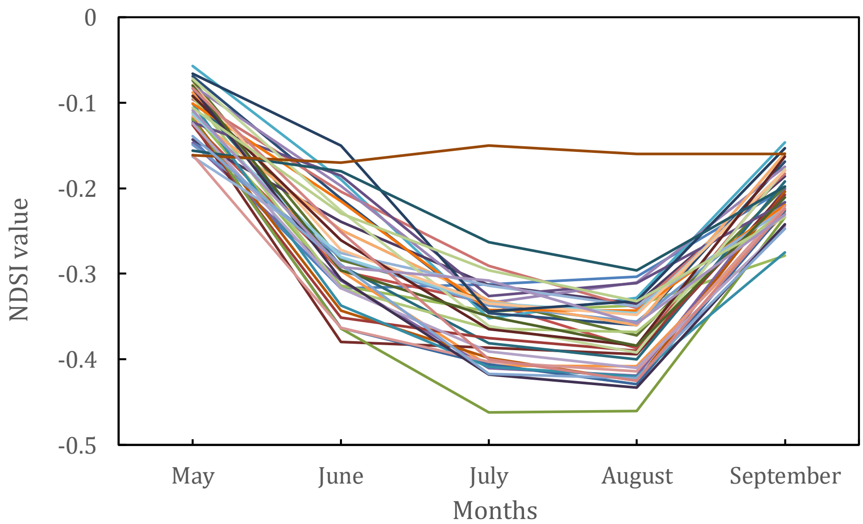

Figure 2. Seasonal variation in NDSI by soil sampling site

Results of statistical analysis and modelling

The results of our linear regression analysis showed a positive relationship between the EC values of the soil samples and the NDSI values derived from satellite images for each month (Figure 3). The R^2 values show a significant and precise relationship ($R^2 = 0.70$) between the soil EC value and the NDSI value obtained from the August satellite image. Based on previous studies by Pankova and Mazikov (1976), it was determined that the optimal shooting time for cotton, particularly in Uzbekistan, is during late summer and early autumn. Pankova and Mazikov (1985) used aerial photographs to determine this, and later published a detailed methodology in 1985 recommending flight dates during this period.

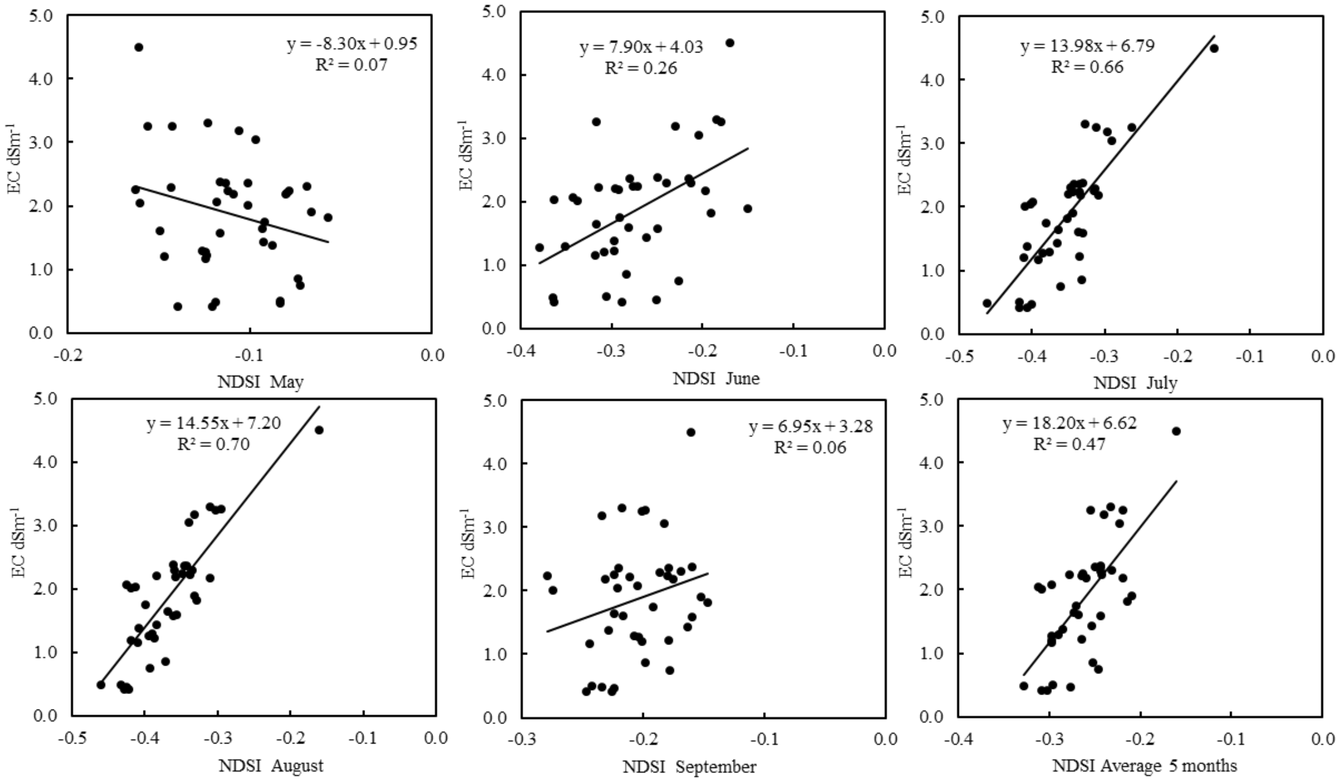

Figure 3. Relationships between EC value and monthly NDSI value

Based on the R^2 values, the order of highest to lowest correlation is as follows: July ($R^2 = 0.66$), the 5-month average ($R^2 = 0.47$), June ($R^2 = 0.26$), May ($R^2 = 0.07$), and September ($R^2 = 0.06$). There are several reasons for the high correlation between August and July. The NDSI index used in the study can be used to detect soil salinity directly. It detects salinity through the visible white salt crusts on the bare soil surface (Ijaz et al., 2020). However, in the remote sensing process, the cotton plant's covering of the soil surface significantly reduces the possibility of detecting salt particles directly on the soil surface using the NDSI index. Nevertheless, NDSI can be used in conjunction with plant reflectance measurements to better understand the spatial distribution and severity of soil salinity (Elhag and Bahrawi, 2017). Salinity-induced stress in cotton plants was determined indirectly in this study using changes in visible and near-infrared reflectors. Based on this, the linear regression analysis results can be divided into binary main factors. The main two factors are the cotton growth stages and the process of soil salinity formation in the study area depending on the period of cotton growth (Figure 4). August has the highest correlation between EC and NDSI, and the first reason for this is the cotton plant's growing season. The cotton plant is planted in the Mingbulak district, which is the research area, in the middle of April, and the vegetation period lasts until the beginning of November (Figure 4).

As a result, cotton's initial development occurs during the months of April, May, and June, when the plant is small and has few leaves. This had an effect on the NDSI values, limiting the plant's ability to separate visible and infrared reflectance. This reduces the possibility of indirect determination of salinity. If we look at the period of cotton growth, the peak of vegetative development corresponds to the end of July and August. During this period, the plant canopy covers a large portion of the pixel surface, appearing as the object with the greatest influence on spectral emissivity, so leaves become the transmitter of soil salinity effects (Salcedo et al., 2022). This indicates that it is the optimal period for determining indirect salinity. Cotton harvest aids involve the use of chemical defoliants to disrupt cotton's physiological and biochemical processes (Chen et al., 2022). Cotton grows and matures faster, and its leaves fall off earlier. Cotton cultivation defoliation activities are carried out in the study region in September. Green leaves begin to dry and fall off as a result. This significantly reduces remote sensing's ability to indirectly determine soil salinity using the example of a cotton plant, as well as the correlation between EC and NDSI for September in this study.

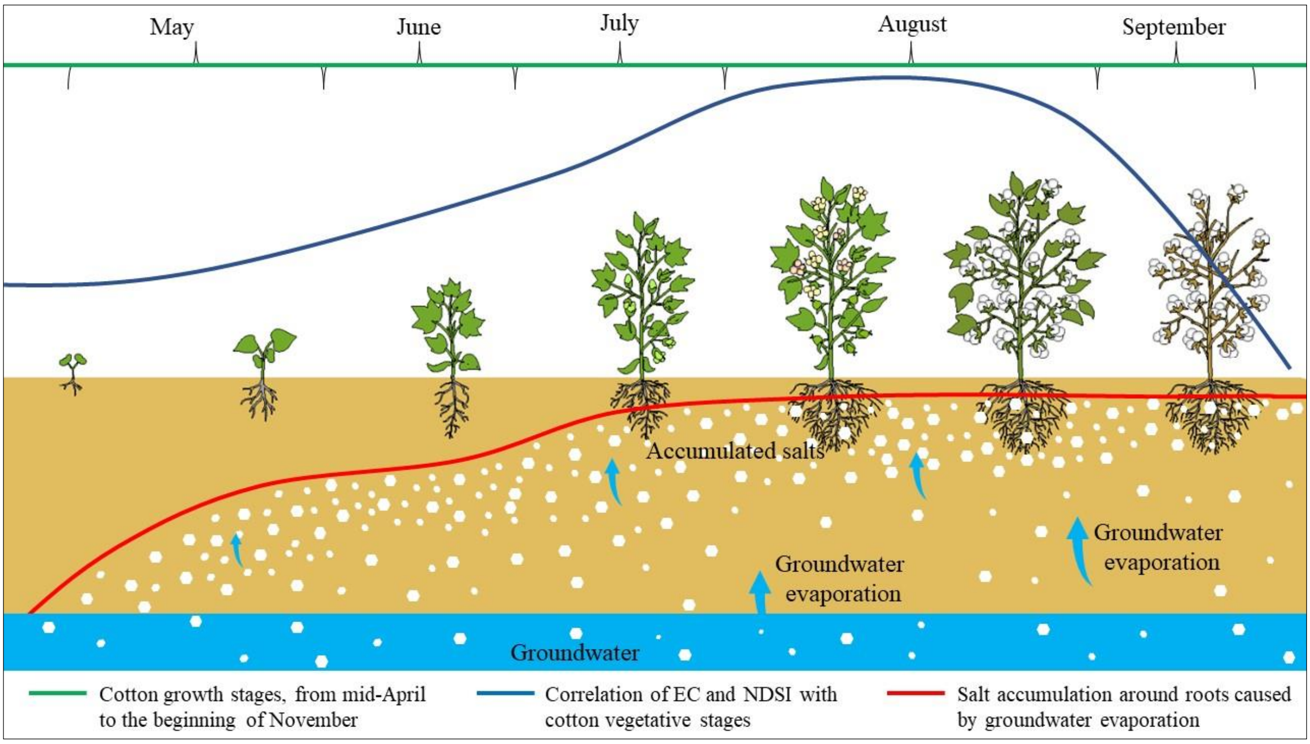

Figure 4. Diagram of seasonal variation in the growth of cotton mulberry and the degree of salt accumulation

As a result, cotton's initial development occurs during the months of April, May, and June, when the plant is small and has few leaves. This had an effect on the NDSI values, limiting the plant's ability to separate visible and infrared reflectance. This reduces the possibility of indirect determination of salinity. If we look at the period of cotton growth, the peak of vegetative development corresponds to the end of July and August. During this period, the plant canopy covers a large portion of the pixel surface, appearing as the object with the greatest influence on spectral emissivity, so leaves become the transmitter of soil salinity effects (Salcedo et al., 2022). This indicates that it is the optimal period for determining indirect salinity. Cotton harvest aids involve the use of chemical defoliants to disrupt cotton's physiological and biochemical processes (Chen et al., 2022). Cotton grows and matures faster, and its leaves fall off earlier. Cotton cultivation defoliation activities are carried out in the study region in September. Green leaves begin to dry and fall off as a result. This significantly reduces remote sensing's ability to indirectly determine soil salinity using the example of a cotton plant, as well as the correlation between EC and NDSI for September in this study.

Although soil samples collected in September were theoretically predicted to have the highest correlation. Another significant aspect is that the mineralogical composition of groundwater is one of the primary causes of salinity in the study area. Cotton fields in the study area are primarily irrigated through furrows, causing groundwater levels to rise. The evaporation of underground water is caused by high temperatures during the summer months (Corwin, 2021; Jahanbazi et al., 2023; Zhang et al., 2023). The maximum temperature in May was 36 °C, 40 °C in June, 41 °C in July, 36 °C in August, and 38 °C in September, according to data from the meteorological station installed in the study area. The evaporation of underground water reached its maximum in July, and as a result, this effect was hidden in August, resulting in the greatest amount of salt accumulating around the plant's roots (Figure 4). Because of the salt accumulation around the roots, the plant's ability to absorb nutrients and water through the roots is limited, resulting in a stress situation in the plant (Kholliyev et al., 2020). As a consequence, it is reasonable to infer that a high accuracy correlation between EC and NDSI was observed in August.

After investigating the relationship between soil salinity and the NDSI index, we used the NDSI to model obtained in August for indirect soil salinity assessment (EC). As a result, the relationship between EC and NDSI was established, as shown in the equations below, with $R^2 = 0.70$:

$$EC = 14.55 \times NDSI + 7.20$$

Using this model, it is possible to deduce the EC level of soils indirectly by remotely analyzing cotton field satellite imagery acquired in the Mingbulak region during August. Although previous studies have used aerial photographs to determine soil salinity, this study utilized more advanced satellite sensors that were not available at the time of those studies. These newer sensors provide more accurate and up-to-date information on soil salinity. Therefore, the findings of this study can be considered an update and improvement on previous research. It is critical to recognize that the outcomes produced by salinity index models are heavily dependent on the various environmental factors present in the study area. As a result, it is plausible to assert that the salinity index and its corresponding models may produce divergent results in different environments.

Conclusion

The relationship between soil salinity and the normalized difference salinity index (NDSI) derived from satellite images was investigated in this study for the Mingbulak region of Uzbekistan. According to the research findings, there is a positive correlation between soil EC values and NDSI values for each month, with pre-flowering and flowering stages August having the highest correlation ($R^2 = 0.70$), as determined by the linear regression analysis.

Furthermore, when analyzing the correlation between EC and NDSI, the study emphasized the importance of accounting for cotton growth stages and the process of soil salinity formation in the study area. The authors determined that August is the best time to use the NDSI index to indirectly determine soil salinity because it corresponds to the peak of vegetative development in the cotton plant, which maximizes the plant's ability to reflect the effects of soil salinity. Additionally, the study proposed a model for indirect soil salinity assessment based on the NDSI index obtained in August, which can be used for remote analysis of cotton field satellite imagery to determine soil EC levels. However, when applying this model in different regions, it is critical to consider environmental factors. Accurately identifying the source of stress, whether salinity, lack of water, or nutrients, is critical for obtaining reliable results in plant stress assessment. The timing of the survey with respect to watering was not specifically addressed in our study which may impact on the interpretation of remote sensing data, and we recognize this as a limitation that will be considered in future studies. It is recommended that irrigation tables be used in conjunction with soil nutrient analysis to achieve greater accuracy. Besides that, the authors intend to improve the precision of their models in future research by collecting soil samples throughout the yearand tracking soil salinity and nutrient levels. This will allow them to create more precise models for assessing soil salinity in agricultural areas. Overall, we found a positive correlation between soil EC values and NDSI values, with the highest correlation found in pre-flowering and flowering stages of cotton. Our results suggest that satellite-based estimation and modeling using NDSI can provide a reliable means of indirectly assessing soil salinity levels in cotton fields. This enables the creation of salinity maps for indirect soil salinity assessment via remote sensing in countries with extensive cotton cultivation, such as Uzbekistan. This approach can potentially save significant time and economic resources compared to traditional soil salinity determination methods.

References

Allbed, A., Kumar, L., 2013. Soil salinity mapping and monitoring in arid and semi-arid regions using remote sensing technology: A Review. *Advances in Remote Sensing* 2(4): 373–385.

Asfaw, E., Suryabhagavan, K.V., Argaw, M., 2018. Soil salinity modeling and mapping using remote sensing and GIS: The case of Wonji sugar cane irrigation farm, Ethiopia. *Journal of the Saudi Society of Agricultural Sciences* 17: 250–258.

Aslanov, I., Kholdorov, S., Ochilov, S., Jumanov, A., Jabbarov, Z., Jumaniyazov, I., Namozov, N., 2021. Evaluation of soil salinity level through using Landsat-8 OLI in Central Fergana valley, Uzbekistan. E3S Web of Conferences 258, 03012.

Chen, P., Xu, W., Zhan, Y., Yang, W., Wang, J., Lan, Y., 2022. Evaluation of cotton defoliation rate and establishment of spray prescription map using remote sensing imagery. *Remote Sensing* 14(17): 4206.

Corwin, D.L., 2021. Climate change impacts on soil salinity in agricultural areas. *European Journal of Soil Science* 72(2): 842-862.

Elhag, M., Bahrawi, J.A., 2017. Soil salinity mapping and hydrological drought indices assessment in arid environments based on remote sensing techniques. *Geoscientific Instrumentation Methods and Data Systems* 6: 149–158.

FAO, 2021. Standard operating procedure for soil electrical conductivity, soil/water, 1:5. FAO, Rome, Italy. 15p. Available at [Access date: 18.05.2023]: https://www.fao.org/3/cb3354en/cb3354en.pdf

Guo, W., Maas, S.J., Bronson, K.F., 2012. Relationship between cotton yield and soil electrical conductivity, topography, and Landsat imagery. *Precision Agriculture* 13: 678–692.

Hamad, I.A., 2016. The use of ınverse distance weighted and fuzzy logic to estimate land suitability by geographic ınformation system in South of Iraq. *Alexandria Science Exchange Journal* 37: 26-35.

Ijaz, M., Ahmad, H.R., Bibi, S., Ayub, M.A., Khalid, S., 2020. Soil salinity detection and monitoring using Landsat data: a case study from Kot Addu, Pakistan. *Arabian Journal of Geosciences* 13: 510.

Ivushkin, K., Bartholomeus, H., Bregt, A.K., Pulatov, A., 2017. Satellite thermography for soil salinity assessment of cropped areas in Uzbekistan. *Land Degradation and Development* 28(3): 870–877.

Jahanbazi, L., Heidari, A., Mohammadi, M.H., Kuniushkova, M., 2023. Salt accumulation in soils under furrow and drip irrigation using modified waters in Central Iran. *Eurasian Journal of Soil Science* 12(1): 63–78.

Khajehzadeh, M., Afzali, S.F., Honarbakhsh, A., Ingram, B., 2022. Remote sensing and GIS-based modeling for predicting soil salinity at the watershed scale in a semi-arid region of southern Iran. *Arabian Journal of Geosciences* 15, 423.

Khan, N.M., Rastoskuev, V. V, Shalina, E. V, Sato, Y., 2001. Mapping Salt-affected Soils Using Remote Sensing Indicators-A Simple Approach With the Use of GIS IDRISI. Proceedings of the 22nd Asian Conference on Remote Sensing, 5-9 November 2001, Singapore. Center for Remote Imaging, Sensing and Processing (CRISP), National University of Singapore; Singapore Institute of Surveyors and Valuers; Asian Association on Remote Sensing, 5 p.

Kholdorov, Sh., Gopakumar, L., Katsura, K., Jabbarov, Z., Jobborov, O., Shamsiddinov, T., Khakimov, A., 2022. Soil salinity assessment research using remote sensing techniques: a special focus on recent research. IOP Conference Series: Earth and Environmental Science 1068: 012037.

Kholdorov, S., Jabbarov, Z., Shamsiddinov, T., 2023a. Soil governance: A review of the current legislative framework for managing soil resources in Uzbekistan. *Soil Security* 13: 100105.

Kholdorov, Sh, Lakshmi, G., Jabbarov, Z., Yamaguchi, T., Yamashita, M., Samatov, N., Katsura, K., 2023b. Analysis of irrigated salt-affected soils in the central Fergana Valley, Uzbekistan, Using Landsat 8 and Sentinel-2 Satellite Images, Laboratory Studies, and Spectral Index-Based Approaches. *Eurasian Soil Science* 56, 1178–1189.

Kholliyev, A., Norboyeva, U., Kholov, Y., Boltayeva, Z., 2020. Productivity of cotton varieties ın soil salinity and water deficiency. *The American Journal of Applied Sciences* 2(10): 7–13.

Li, Y., Chang, C., Wang, Z., Zhao, G., 2022. Remote sensing prediction and characteristic analysis of cultivated land salinization in different seasons and multiple soil layers in the coastal area. *International Journal of Applied Earth Observation and Geoinformation* 111: 102838.

Liu, Y., Zhang, F., Wang, C., Wu, S., Liu, J., Xu, A., Pan, K., Pan, X., 2019. Estimating the soil salinity over partially vegetated surfaces from multispectral remote sensing image using non-negative matrix factorization. *Geoderma* 354: 113887.

Metternicht, G.I., Zinck, J.A., 2003. Remote sensing of soil salinity: Potentials and constraints. *Remote Sensing of Environment* 85(1): 1-20.

Pankova E.I., Mazikov V.M., 1985. Guidelines for the use of aerial photography materials for assessing soil salinity and conducting salt surveys of irrigated areas of the cotton-growing zone on a large and medium scale. Moscow, Russia. 73p. [in Russian].

Pankova E.I., Mazikov V.M., 1976. Estimation of salinity of irrigated soils of cotton fields from aerial photographs (on the example of the Golodnoy Steppe). Pochvvedenie 5: 55–65. [in Russian].

Salcedo, F.P., Cutillas, P.P., Cabañero, J.J.A., Vivaldi, A.G., 2022. Use of remote sensing to evaluate the effects of environmental factors on soil salinity in a semi-arid area. *Science of The Total Environment* 815: 152524.

Scudiero, E., Skaggs, T.H., Corwin, D.L., 2015. Regional-scale soil salinity assessment using Landsat ETM+ canopy reflectance. Remote Sensing of Environment 169: 335–343.

Stavi, I., Thevs, N., Priori, S., 2021. Soil salinity and sodicity in drylands: A review of causes, effects, monitoring, and restoration measures. *Frontiers in Environmental Science* 9: 712831.

Tan, J., Ding, J., Han, L., Ge, X., Wang, X., Wang, J., Wang, R., Qin, S., Zhang, Z., Li, Y., 2023. Exploring planetscope satellite capabilities for soil salinity estimation and mapping in arid regions oases. *Remote Sensing* 15(4): 1066.

Richards, L.A., 1954. Diagnosis and improvement of saline and alkaline soils. Agriculture Handbook, Vol. 60, USDA, Washington DC, 160 p.

Vaughn, I., 2019. Landsat 8 (L8) Data Users Handbook. USGS Science for a Changing World. EROS, Sioux Falls, South Dakota. 106p.

Wiegand, C.L., Rhoades, J.D., Escobar, D.E., Everitt, J.H., 1994. Photographic and videographic observations for determining and mapping the response of cotton to soil salinity. *Remote Sensing of Environment* 49(3): 212-223.

Zafar, M.M., Shakeel, A., Haroon, M., Manan, A., Sahar, A., Shoukat, A., Mo, H., Farooq, M.A., Ren, M., 2022. Effects of salinity stress on some growth, physiological, and biochemical parameters in cotton (Gossypium hirsutum L.) germplasm. *Journal of Natural Fibers* 19(14): 8854–8886.

Zhang, J., Zhang, Z., Chen, J., Chen, H., Jin, J., Han, J., Wang, X., Song, Z., Wei, G., 2021. Estimating soil salinity with different fractional vegetation cover using remote sensing. *Land Degradation and Development* 32(2): 597–612.

Zhang, X., Shu, C., Wu, Y., Ye, P., Du, D., 2023. Advances of coupled water-heat-salt theory and test techniques for soils in cold and arid regions: A review. *Geoderma* 432: 116378.

Zhang, Y., Hou, K., Qian, H., Gao, Y., Fang, Y., Xiao, S., Tang, S., Zhang, Q., Qu, W., Ren, W., 2022. Characterization of soil salinization and its driving factors in a typical irrigation area of Northwest China. Science of the Total Environment 837: 155808.

Zhu, K., Sun, Z., Zhao, F., Yang, T., Tian, Z., Lai, J., Zhu, W., Long, B., 2021. Relating hyperspectral vegetation indices with soil salinity at different depths for the diagnosis ofwinter wheat salt stress. *Remote Sensing* 13(2): 250.

Zörb, C., Geilfus, C.M., Dietz, K.J., 2019. Salinity and crop yield. *Plant Biology* 21(S1): 31-38.